Journal of Ceramic Processing Research. Vol. 13, No. 4, pp. 491~494 (2012)

J O U R N A L O F
Ceramic Processing Research

Carbon nanofibers combined with Pt nanoparticles for use as counter electrodes in dye-sensitized solar cells

Suk In Noh[a], Tae-Yeon Seong[b,*] and Hyo-Jin Ahn[a,*]

[a]*Department of Materials Science & Engineering, Seoul National University of Science and Technology, Seoul 139-743, Korea*
[b]*Department of Materials Science & Engineering, Korea University, Seoul 136-713, Korea*

Carbon nanofibers (CNFs) combined with different amounts of Pt nanoparticles (CNF/Pt nanocomposites) were syntheiszed by a combination of electrospinning and precipitation methods. Their structural and morphological properties were investiaged by means of scanning electron microscopy, transmission electron microscopy, X-ray diffraction, and X-ray photoelectron spectroscopy. Dye-sensitized solar cells (DSSCs) fabricated with CNF/Pt nanocomposites (with 40 wt% Pt nanoparticles) exhibit a much better short-circuit current density (13.54 mA/cm^2), fill-factor (49.81%), and photoconversion efficiency (4.47%) than do those with CNF only and CNF/Pt nanocomposites (with 20 wt% Pt nanoparticles). It is also shown that dye-sensitized solar cells (DSSCs) fabricated with CNF/Pt nanocomposites (with 40 wt% Pt nanoparticles) show almost the same cell efficiency as that of DSSCs with a commercial pure Pt-sol sample.

Key words: Compoistes, Carbon nanofiber, Pt nanoparticles, Electrospinning, Dye-sensitized solar cells.

Introduction

Dye-sensitized solar cells (DSSCs), being considered as an alternative device of conventional p-n junction solar cells, are of considerable interest because of their high conversion efficiency, low cost, simple assembly process, and various industrial applications [1-7]. DSSCs are composed of n-type nano-porous semiconductor particles (e.g., TiO_2 and ZnO nanoparticles, whose surfaces were chemically absorbed with solar-energy absorbing sensitizers) for a working electrode, iodine electrolyte, and platinum (Pt) catalyst for a counter electrode. Recent scientific issues in DSSCs are the development of low-temperature fabrication methods, semiconductor quantum dot sensitizers, and low-cost materials for replacing the Pt catalyst (namely, the counter electrode) [8-10]. In the case of counter electrodes in DSSCs, Pt is the most commonly used catalyst because of its good electrical conductivity and long-term stability in an electrolyte during a redox reaction [11]. However, Pt is a rare metal and very expensive. Thus, if low-cost alternative electrodes could be developed, the conversion rate cost of DSSCs would go down to \$0.4/W_P or less [12]. For this reason, studies on alternatives to replace Pt catalysts for use as counter electrodes in DSSCs have been actively carried out. For example, Sea-Fue et al. reported that DSSCs fabricated with nitrogen-doped diamond-like carbon films for counter electrodes exhibited an energy conversion efficiency of 3.35% [13]. Ko *et al*. reported that DSSCs fabricated with tungsten carbide particles as a non-Pt counter electrode showed an energy conversion efficiency of 3.03% at a reaction temperature of 800 °C [14]. Wenjing *et al*. synthesized graphene/PEDOT-PSS composite films for counter electrodes in DSSCs and reported a conversion efficiency of 4.5% [15]. However, the photovoltaic properties of carbon nanofibers (CNFs) combined with Pt nanoparticles for counter electrodes in cost-effective DSSCs have not been studied hitherto.

In this study, in order to investigate counter electrodes for use in DSSCs, CNFs combined with Pt nanoparticles were synthesized by a combination of electrospinning and precipitation methods and their structural and photovoltaic properties were investigated as a function of the Pt content. CNFs were used as a supporting material because of their advantages, such as high tensile strength, high specific surface area, and good electrical conductivity [16]. Furthermore, the photovoltaic properties of DSSCs fabricated with CNFs combined with Pt nanoparticles are compared to that of DSSCs with a commercial pure Pt-sol sample.

Experimental procedures

CNFs were prepared by an electrospinning method. Polyacrylonitrile (PAN, M_w = 150,000 g/mol, Aldrich) as a carbon precursor and poly(vinylpyrrolidone) (PVP, M_w = 1,300,000 g/mol, Aldrich) as a stabilizer of the solvent were used so as to fabricate CNFs. A PAN and PVP-dissolved in N,N-dimethylformamide (DMF, Aldrich) solution was prepared at room temperature.

*Corresponding author:
Tel : +82-2-3290-3288 ; +82-2-970-6622
Fax: +82-2-3290-3288 ; +82-2-973-6657
E-mail: tyseong@korea.ac.kr ; hjahn@seoultech.ac.kr

Then the as-prepared solution was loaded into a 12 ml plastic syringe equipped with a 23-gauge stainless needle. The distance between the needle tip and collector was fixed at ~15 cm under a supply voltage of 11 kV and the feeding rate during electrospinning was maintained at ~0.04 ml/h. The calcination of the resulting polymer fibers was conducted by a two step process. In the first step, the resulting polymer fibers were annealed at 230 °C for 5 h in a tube-furnace for stabilization. Then, carbonization was carried out at 800 °C for 1 h in an N_2 ambient. In order to synthesize CNFs combined with Pt nanoparticles, the electro-spun CNFs were dispersed in a nitric acid solution mixed with de-ionized (DI) water for 12 h and then the CNFs were rinsed by DI water several times. The CNFs were first dispersed again in DI water for 6 h, after which ethylene glycol mixed with H_2PtCl_6 (Aldrich) was added and stirred for 0.5 h. $NaBH_4$ (Aldrich) (a reducing agent) was added to the above-mentioned solution for a reduction reaction. Two different types of CNFs combined with Pt nanoparticles were fabricated: for the first, 0.086 M H_2PtCl_6 in ethylene glycol and 4.7 M $NaBH_4$ in DI water were used and for the second, 0.172 M H_2PtCl_6 in ethylene glycol and 9.4 M $NaBH_4$ in DI water were used, after which they were freeze-dried at -50 °C. This resulted in the synthesis of CNFs combined with 20 and 40 wt% Pt nanoparticles (referred to here as sample A and sample B, respectively). For comparison, CNF only electrodes were also prepared. Fig. 1 shows a schematic diagram of the synthesis process of CNFs combined with Pt nanoparticles (referred to here as CNF/Pt nanocomposites). The paste for a counter electrode containing CNFs (sample A or B), carboxymethyl cellulose sodium salt (CMC, Mw = ~90,000 g/mol, Aldrich), and DI water were ground in an alumina mortar. The resulting paste was squeeze-printed on fluorine-doped tin oxide coated glasses (FTO, 15 Ω/cm^2, Pilkington). These samples were then dried at 80 °C for 6 h and sintered at 200 °C for 0.5 h in air. In the case of the working electrode, TiO_2 paste consisting of P25 (Degussa), hydroxypropyl cellulose (HPC, M_w ~ 80,000, Aldrich), acetyl acetone (Aldrich), and DI water was used. TiO_2 paste-printed FTO glasses were immersed into a 0.5 mM $Ru(dcbpy)_2(NCS)_2$ (N719, Solaronix) solution for 24 h. A 0.3 M DMPII-based iodine solution was used as an electrolyte [16].

The morphologies of the samples were examined by field-emission scanning electron microscopy (FESEM, Hitachi S-4700) and transmission electron microscopy (TEM, TECNAI-F20). The crystal structures and chemical bonding states of the samples were analyzed by X-Ray diffraction (XRD, Rigaku Rint 2500 with a Cu K_α radiation) and X-ray photoemission spectroscopy (XPS, ESCALAB 250 with an Al Kα X-ray source). The photovoltaic properties of DSSCs were examined under standard irradiation (AM 1.5 simulated sunlight) with a light intensity of 100 mA/cm^2 using a 150 watt xenon lamp (LAB 50).

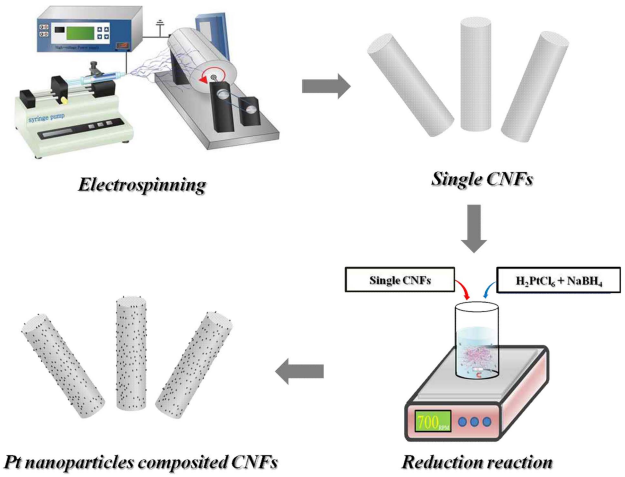

Fig. 1. A schematic diagram of the formation process of CNFs combined with Pt nanoparticles for a counter electrode in DSSCs, which were synthesized by combining electrospinning and precipitation methods.

Results and Discussion

Fig. 2 shows SEM images obtained from the CNFs only sample, sample A, and sample B. For the CNFs only sample, Fig. 2(a), CNFs are measured to be in the range of 140 - 160 nm in diameter. It is noted that sample A and sample B, as shown in Figs. 2(b) and 2(c), reveal relatively rougher surfaces than does the CNFs only sample. This is believed to be due to the presence of the Pt nanoparticles.

To characterize if Pt nanoparticles are properly incorporated into CNFs, all the samples were examined by TEM. Fig. 3 shows TEM bright-field images obtained from the CNFs only sample, sample A and sample B. For the CNFs only sample (Fig. 3(a)), the TEM image shows that CNFs have a uniform contrast. A CNF is

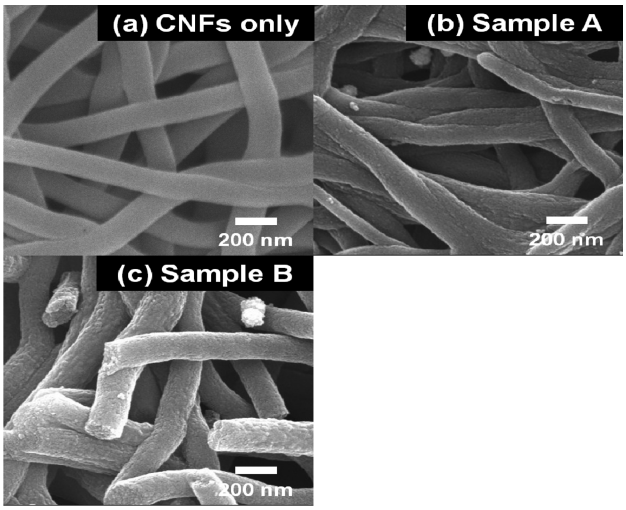

Fig. 2. SEM images obtained from (a) CNFs only sample, (b) sample A and (c) sample B after calcination at 800 °C for 1 h.

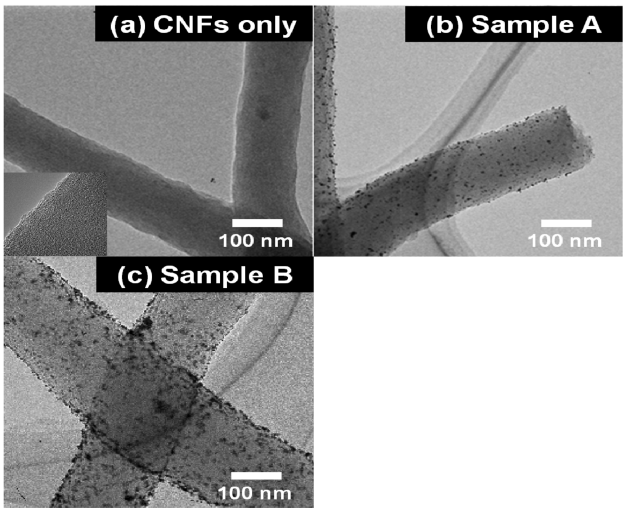

Fig. 3. TEM bright field images obtained from (a) CNFs only sample, (b) sample A and (c) sample B after calcination at 800 °C for 1 h.

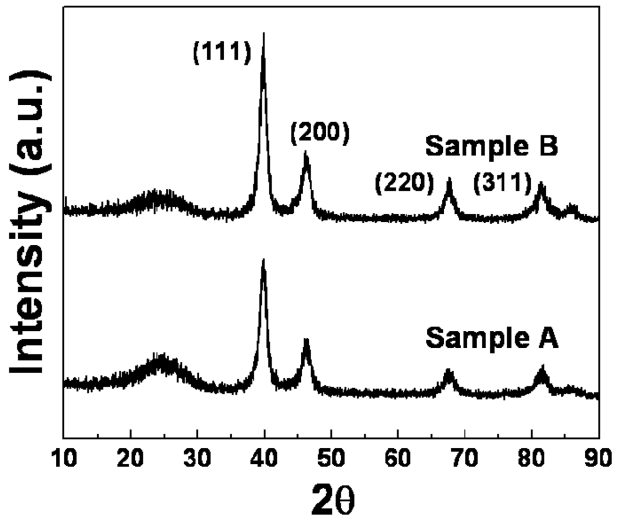

Fig. 4. Powder XRD plots obtained from sample A and sample B.

shown enlarged in the inset (left bottom) of Fig. 3(a), exhibiting its amorphous characteristic. For sample A and sample B, the TEM images reveal dark blobs that are ~3 - 7 nm in size and rather well distributed across the whole CNFs. The dark blobs are believed to be Pt nanoparticles. It is noted that sample B (Fig. 3(c)) exhibits a higher density of the Pt nanoparticles than does sample A (Fig. 3(b)).

Fig. 4 shows powder XRD plots obtained from sample A and sample B. The XRD results exhibit characteristic diffraction peaks at 39.7 °, 46.2 °, 67.4 ° and 81.2 °, corresponding to the (111), (200), (220) and (311) planes (respectively,) of the face-centered cubic structure of the polycrystalline Pt phase (space group *fm3m* [225]) (JCPDS card No. 04-0802). On the basis of the diffraction peaks, the size of the Pt nanoparticles can be calculated by the Scherrer equation given below [17]:

$$D = 0.9\lambda/(\beta\cos\theta) \quad (1)$$

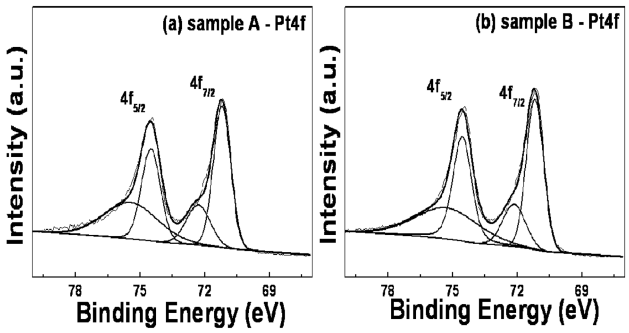

Fig. 5. XPS Pt $4f_{5/2}$ and $4f_{7/2}$ core level spectra of (a) sample A and (b) sample B.

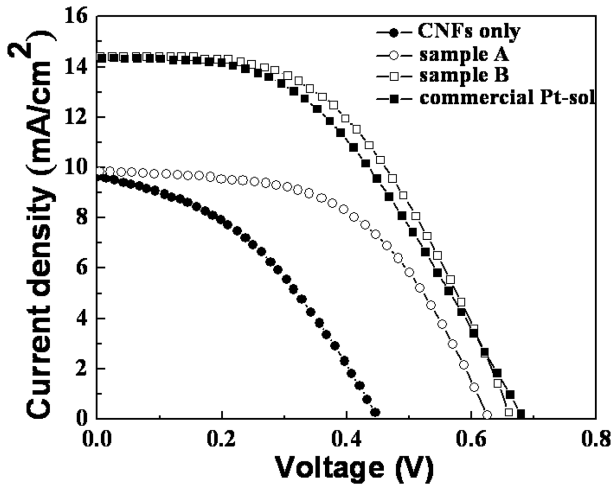

Fig. 6. Photocurrent density (J) - voltage (V) data measured from DSSCs fabricated with the CNFs only sample, sample A, sample B and a commercial Pt-sol sample.

where λ is the X-ray wavelength, β is the full width at half maximum (FWHM) and θ is the Bragg angle. The average sizes of the Pt nanoparticles were estimated to be ~5.5 nm. This is in good agreement with those measured by the TEM examination. In addition, there are broad diffraction peaks at ~25.0 °. These peaks are believed to be due to the CNFs, indicating the amorphous nature of the CNFs. The SEM, TEM, and XRD results show that sample A and sample B are composed of polycrystalline Pt nanoparticles and amorphous CNFs, namely, a successful synthesis of amorphous CNFs combined with Pt nanoparticles.

In order to examine the chemical bonding states of Pt atoms, XPS examinations were performed on sample A and sample B. Fig. 5 exhibits XPS spectra for the Pt $4f_{5/2}$ and Pt $4f_{7/2}$ photoelectrons observed at ~74.5 and ~71.2 eV, respectively [18]. This implies that the elemental Pt is present as a zero-valent metallic state. In addition, the other two peaks observed at ~75.5 and ~72.3 eV are related to the Pt (II) states, such as $Pt(OH)_2$, as previously reported by Ahn et al. [19]. However, in spite of the existence of the Pt (II) states, the Pt nanoparticles in the CNFs are mainly present as metallic phases, as shown in Figs. 5(a) and 5(b).

Fig. 6 shows the photocurrent density (*J*)-voltage (*V*)

curves obtained from the CNFs only sample, sample A, and sample B for counter electrodes in DSSCs. For comparison, commercial pure Pt-sol (Solaronix) samples were also investigated. Measurements show that short-circuit current densities (J_{sc}) for the CNFs only sample, sample A, sample B, and the commercial pure Pt-sol sample are 9.05, 9.24, 13.54 and 14.33 mA/cm^2, respectively. The open-circuit voltages (V_{oc}) for the CNFs only sample, sample A, sample B, and the commercial pure Pt-sol sample are estimated to be 0.45, 0.62, 0.66 and 0.68 V, respectively. These results indicate that the short-circuit current densities (J_{sc}) and open-circuit voltage (V_{oc}) of DSSCs are improved with an increase in the amount of Pt nanoparticles. In addition, fill factors (*ff*) for the CNFs only sample, sample A, sample B, and the commercial pure Pt-sol are 40.06, 53.54, 49.81, and 45.26%, respectively. It is noteworthy that sample A and sample B yield higher fill factors (*ff*) as compared to the CNFs only and commercial pure Pt-sol samples. The photoconversion efficiency (PCE, η) for all the samples can be calculated by the equation given below [2]:

$$\eta\ (\%) = [J_{sc} \times V_{oc} \times ff]/[I_{max} \times V_{max}] \quad (2)$$

where J_{sc} is the short-circuit photocurrent density, V_{oc} is the open-circuit voltage, *ff* is the fill factor, I_{max} is a maximum value of the power current, and V_{max} is a maximum value of the power voltage. Consequently, the photoconversion efficiencies (η) for the CNFs only sample, sample A, sample B, and the commercial pure Pt-sol sample were estimated to be 1.64, 3.11, 4.47 and 4.44%, respectively. It is noted that the photoconversion efficiency of sample B is superior to those of the CNFs only and sample A. It is worth noting that despite a far less amount of Pt in sample B, its photoconversion efficiency is almost the same as that of the commercial pure Pt-sol sample. Therefore, the enhanced photoconversion efficiency of sample B can be attributed to the improved electrocatalytic activity with the I^-/I_3^- electrolyte due to the presence of well-distributed Pt nanoparticles on the CNFs. The CNFs combined with Pt nanoparticles can serve as a promising counter electrode for the fabrication of highly efficient and cost-effective DSSCs.

Conclusions

CNFs combined with Pt nanoparticles (CNF/Pt nanocomposites) for use in a counter electrode in DSSCs were successfully fabricated by combining electrospinning and precipitation methods. The SEM, TEM, XRD and XPS results showed that the CNF/Pt nanocomposites consisted of polycrystalline Pt nanoparticles (3 - 7 nm across) and amorphous CNFs. DSSCs fabricated with CNF/Pt nanocomposites (with 40% Pt nanoparticles: sample B) showed a higher photoconversion efficiency than did the CNFs only sample, sample A, and a commercial pure Pt-sol sample. Considering the fact that sample B contains a lesser amount of Pt than the commercial pure Pt-sol sample, CNF/Pt nanocomposites can serve as a promising counter electrode for the fabrication of highly efficient and cost-effective DSSCs.

Acknowledgement

This work was supported by Grant No. 10031768 from the Ministry of Knowledge Economy (MKE) and Fundamental R&D Program for Core Technology of Materials funded by the Ministry of Knowledge Economy, Republic of Korea.

References

1. M. Grätzel, Nature 414 (2001) 338-344.
2. M. Grätzel, J. Photochem. Photobiol. C4 (2003) 145-153.
3. L. Han, N. Koide, Y. Chiba and T. Mitate, Appl. Phys. Lett. 84 (2004) 2433-2435.
4. M. Dürr, A. Bamedi, A. Yasuda and H. Nelles, Appl. Phys. Lett. 84 (2004) 3397-3399.
5. G. Smestad, C. Bignozzi and R. Argazzi, Sol. Energy Mater. Sol. Cells 32 (1994) 259-272.
6. S. Dai, K. Wang, J. Weng, Y. Sui, Y. Huang, S. Xiao, S. Chen, L. Hu, F. Kong, X. Pan, C. Shi and L. Guo, Sol. Energy Mater. Sol. Cells 85 (2005) 447-455.
7. S. K. Deb, Sol. Energy Mater. Sol. Cells 88 (2005) 1-10.
8. K.-K. Kim, G.-W. Lee, K.-C. Yoo, D.-Y. Kim, J.-K. Kim and N.-G. Park, J. Photochem. Photobio. A 204 (2009) 144-147.
9. J.-H. Im, C.-R. Lee, J.-W. Lee, S.-W. Park and N.-G. Park, The Royal Society of Chemistry, (2011) (in press).
10. Takurou N. Murakami, S. Ito, Qing Wang, Md. Khaja Nazeeruddin, Takeru Bessho, I. Cesar, P. Liska, R. Humphry-Baker, P. Comte, P. Péchy and M. Grätzel, J. Electrochem. Soc. 153 (2006) A2255-2261.
11. R. Pellicano, M. Iannantuono, A. Di Ciommo, M. Bisceflia and M. Grätzel, A. Key, Sol. Energy Mater. Sol. Cells 44 (1996) 99-117.
12. G. Hashmi, K. Miettunen, T. Peltola, J. Halme, I. Asghar, K. Aitola, M. Toivola and P. Lund, Renewable and Sustainable Energy Reviews 15 (2011) 3717-3732.
13. W. Sea-Fue, K. Koteswara Rao, T.C.K. Yang and W. Hsin-pei, J. Alloy. Compd. 509 (2011) 1969-1974.
14. A.-R. Ko, J.-K. Oh, Y.-W. Lee, S.-B. Han and K.-W. Park, Mater. Lett. 65 (2011) 2220-2223.
15. H. Wenjinh, X. Wuxi, L. Gewu, L. Chun and S. Gaoquan, Electrochem. Commun. 10 (2008) 1555-1558.
16. H.-S. Lee, S.-H. Bae, Y. Jo, K.-J. Kim, Y. Jun and C.-H. Han, Electrochim. Acta 55 (2010) 7159-7165.
17. H.-J. Ahn, H.-C. Choi, K.-W. Park, S.-B. Kim and Y.-E. Sung, J. Phys. Chem. B 108 (2004) 9815-9820.
18. J.F. Moulder, W.F. Stickle, P.E. Sobol and K.D. Bomben, Handbook of X-ray Photoelectron Spectroscopy, Physical Electronics, Eden Pairie, MN, 1995.
19. H.-J. Ahn, H.-S. Shim, W.B. Kim, Y.E. Sung and T.-Y. Seong, J. Alloy. Compd. 471 (2009) L39-L42.